MOLECULAR AND CELLULAR BIOLOGY, Jan. 2006, p. 77–87 Vol. 26, No. 1
0270-7306/06/$08.00+0 doi:10.1128/MCB.26.1.77–87.2006

Defects in Yolk Sac Vasculogenesis, Chorioallantoic Fusion, and Embryonic Axis Elongation in Mice with Targeted Disruption of *Yap65*

Elizabeth M. Morin-Kensicki,[1,2]†* Brian N. Boone,[1]† Michael Howell,[1] Jaclyn R. Stonebraker,[3] Jeremy Teed,[1] James G. Alb,[1] Terry R. Magnuson,[2] Wanda O'Neal,[3] and Sharon L. Milgram[1,3]

Department of Cell and Developmental Biology, CB7090, University of North Carolina at Chapel Hill, Chapel Hill, North Carolina 27599-7090[1]; Department of Genetics, CB7264, University of North Carolina at Chapel Hill, Chapel Hill, North Carolina 27599-7264[2]; and Cystic Fibrosis/Pulmonary Research and Treatment Center, CB7248, University of North Carolina at Chapel Hill, Chapel Hill, North Carolina 27599-7248[3]

Received 6 May 2005/Returned for modification 10 July 2005/Accepted 8 October 2005

YAP is a multifunctional adapter protein and transcriptional coactivator with several binding partners well described in vitro and in cell culture. To explore in vivo requirements for YAP, we generated mice carrying a targeted disruption of the *Yap* gene. Homozygosity for the *Yap*^{tm1Smil} allele (*Yap*$^{-/-}$) caused developmental arrest around E8.5. Phenotypic characterization revealed a requirement for YAP in yolk sac vasculogenesis. Yolk sac endothelial and erythrocyte precursors were specified as shown by histology, PECAM1 immunostaining, and *alpha globin* expression. Nonetheless, development of an organized yolk sac vascular plexus failed in *Yap*$^{-/-}$ embryos. In striking contrast, vasculogenesis proceeded in both the allantois and the embryo proper. Mutant embryos showed patterned gene expression domains along the anteroposterior neuraxis, midline, and streak/tailbud. Despite this evidence of proper patterning and tissue specification, *Yap*$^{-/-}$ embryos showed developmental perturbations that included a notably shortened body axis, convoluted anterior neuroepithelium, caudal dysgenesis, and failure of chorioallantoic fusion. These results reveal a vital requirement for YAP in the developmental processes of yolk sac vasculogenesis, chorioallantoic attachment, and embryonic axis elongation.

Yes-associated protein (YAP65; referred to as YAP throughout) is a modular adapter protein first identified as a binding partner for the product of the proto-oncogene c-*Yes* (57). YAP contains multiple protein interaction domains, including a proline-rich amino terminus, a 14-3-3 binding site (3), WW domains (32, 57), SH3 binding motifs (12, 57), a coiled-coil, and a consensus PDZ binding motif at the extreme COOH terminus (43). YAP mRNA is broadly distributed, and expressed sequence tags have been identified in cDNA libraries from many different species and from many tissues, cell lines, and tumor samples. Although the cellular and subcellular localization of the YAP protein has been less well characterized, it is expressed in multiple cell types and can be localized to both cytoplasmic and nuclear compartments (3, 26, 32, 45, 60, 64, 69). This broad distribution and the modular structure of YAP together suggest multiple cellular functions.

The identification of YAP-interacting proteins has provided insight into potential roles for YAP in cell signaling within both cytosol and nucleus. YAP cytosolic interactions may impact cell signaling pathways by several possible mechanisms. For example, YAP binds the SH3 domain of c-Yes (57) and can also associate with cytoplasmic PDZ proteins via its COOH terminus (43). Therefore, YAP may play a role in the anchoring and/or targeting of c-Yes to position the kinase to respond to specific extracellular cues or to phosphorylate specific cellular substrates. Cytosolic YAP also may modulate growth factor receptor signaling. For example, YAP associates with the inhibitory Smad7 to attenuate transforming growth factor β signaling (14) and may affect signaling via the ErbB-4 receptor (32, 45). In the nucleus, YAP may function as a coregulator, modulating the activity of several transcription factors. In this manner, YAP interacts with RUNX family members (64, 69), which impact hematopoiesis and osteogenesis, as well as TEAD family members (39, 60), which are implicated in muscle cell and neural crest cell differentiation. Furthermore, we recently found that the proline-rich amino terminus of YAP associates in the nucleus with heterogeneous nuclear ribonucleoprotein U (26), a protein involved in mRNA processing and the control of gene expression. Finally, several pieces of data argue that regulated localization of YAP may impact apoptosis and cell cycle progression. Indeed, in the nucleus the YAP WW domain associates directly with the p53 gene family members p73α, p73β, and p63α and enhances the transcription of proapoptotic *Bax* and *Mdm2* reporter constructs and endogenous *Bax* (55). In addition, phosphorylation by Akt stimulates YAP interaction with cytosolic 14-3-3 and attenuates p73-mediated apoptosis (55). YAP may also associate with p53BP2 (12), a protein known to inhibit the activity of the p53 tumor suppressor. Thus, YAP likely exists in cell type- and compartment-specific protein complexes that define its function throughout development and in the adult organ-

* Corresponding author. Mailing address: 510 Taylor Hall, CB7090, Department of Cell and Developmental Biology, University of North Carolina at Chapel Hill, Chapel Hill, NC 27599-7090. Phone: (919) 966-0389. Fax: (919) 966-1856. E-mail: emkunc@med.unc.edu.

† E.M.M.-K. and B.N.B contributed equally to this study.

ism, and yet specific in vivo requirements for YAP remain undefined.

YAP shows significant similarity to the product of the related gene, *Taz* (30). With amino acid identity approaching 50%, YAP and TAZ may share common protein partners, and yet distinctions have been described (8, 21, 25, 26, 30, 37, 47) The extent to which these proteins show unique or overlapping function in vivo remains unclear. Thus, the potential for redundancy between these proteins emphasizes the probable complexity of YAP function and highlights the need for understanding in vivo requirements for YAP.

Although an integrated view of YAP protein interactions and function is lacking, the data suggest that YAP is an adaptor protein that modulates multiple signal transduction pathways in many cell types. These pathways have been explored in biochemical assays and in cell culture model systems, but little is known regarding YAP function in the intact organism. To investigate in vivo requirements for YAP, we generated mice carrying a targeted disruption in the *Yap* gene. The embryonic lethal phenotype of homozygous mutant mice indicates that YAP is essential for embryogenesis and that, in fundamental developmental events, TAZ does not compensate for YAP. These results demonstrate for the first time a critical role for YAP in early embryonic development.

MATERIALS AND METHODS

Generation of the *Yap^{tm1Smil}* allele. A 507-nucleotide (nt) probe generated by PCR amplification from a mouse lung cDNA library (primer pair 5′-AGTTTC TGTCTCAGTTGGGACG-3′ [nt 13 to 34 of accession X80508] and 5′-CAT GCTGTGGAGTGAGAGGCTC-3′ [nt 520 to 500 of X80508]) was used to screen a 129SvEv mouse genomic library packaged in Lambda Gem-ll with 13- to 15-kb inserts. Two of nine plaques subcloned into pBluescript SK (Stratagene) and partially sequenced provided genomic DNA sequence for the *Yap* targeting vector construct. The targeting vector 5′ arm of homology was generated by using a phage HindIII to mouse HindIII 1.3-kb fragment as genomic sequence upstream of the *Yap* coding sequence. The targeting vector 3′ arm of homology was generated by using a *Yap* exon 1 internal XhoI to phage XhoI 7.0-kb fragment that encompassed *Yap* exon 2 and downstream sequence. Subcloning these into HindIII and XhoI cloning sites of the pOSdupdel6142-SA vector (kindly provided by the UNC Animal Models Core) generated the targeting vector pOSdupdel6142-Yap65. The targeting vector replaces about 1 kb of genomic sequence with a reverse orientation, floxed *MC1-neo* cassette, and appends a *PGK-TK* cassette for negative selection.

Vector electroporation into 129SvEv embryonic stem (ES) cells and selection with Geneticin and ganciclovir, followed by PCR screening and Southern blot confirmation identified six ES cell clones with the targeted recombination event. ES cells from two expanded clones were injected into C57BL/6J blastocysts to generate chimeric founders. Founder males from each ES cell line were crossed to C57BL/6J female mice to give *Yap^{tm1Smil}* mice heterozygous for the targeted allele that then were crossed to initiate *Yap^{tm1Smil}* lines. We used allele nomenclature according to the guidelines established by the International Committee on Standardized Genetic Nomenclature for Mice and as implemented by the Mouse Genomic Nomenclature Committee. All ES cell work and generation of chimeric animals was conducted in the UNC Animal Models Core Facility according to well-established and approved protocols.

NCBI Build 33.1 of the mouse genome, released on 3 September 2004 (http://www.ncbi.nlm.nih.gov/mapview/map_search.cgi?taxid = 10090), indicated a putative locus, *loc434366*, identified by the gene recognition program GNOMON and in opposing orientation to the *Yap* gene that also is perturbed in this allele. The possible existence of a transcribed gene at this locus is supported by in silico identification of a promoter signal on that strand using promoter recognition computer algorithms (09/01/2004, McPromoter, http://genes.mit.edu/McPromoter.html; 09/01/2004, www promoter scan, http://bimas.dcrt.nih.bov/cgi-bin/molbio/proscan; 09/01/2004, Promoter 2.0, http://www.cbs.dtu.dk/services/Promoter/output.php) and by a single expressed sequence tag (accession CB600667) from the kidney cDNA library 12886: NIH_MGC_176. If translated, this gene would produce a highly unusual 95-amino-acid protein consisting largely of glutamic acid and lysine repeats. Nonetheless, to assess the potential impact on our further studies of having also disrupted this locus, we generated PCR primers in predicted *loc434366* exons 2 and 3 (sequence below) and examined possible expression by reverse transcription-PCR (RT-PCR). This primer pair generates a 433-nt amplicon from reverse-transcribed RNA sequence but covers 3.2 kb of genomic sequence. We examined expression of *loc434366* in a mouse kidney cDNA library (Stratagene) and in wild-type embryos at specific stages ranging from blastocyst (embryonic day 3.5 [E3.5]) stage to late gestation (E18.5) and found expression in kidney but no detectable expression in embryos until after E7.5 (data not shown).

Genotyping. ES cells, mice, and tissue scrapings from paraffin sections were genotyped by either Southern blot or PCR-based methods. We generated a 542-nt Southern probe by PCR amplification from subcloned genomic sequences 5′ to the *Yap* targeting construct using the primer pair 5′-GCTGCCATTTCA ACTTTCTAC-3′ and 5′-CAGCAGTCTATCGCTTTGTG-3′. This probe recognizes an approximately 6-kb fragment from genomic DNA and an approximately 5-kb fragment from the targeted allele after enzymatic digestion with BamHI. To genotype by PCR, we used a primer trio that included a shared 5′ primer from sequence upstream of the *Yap* gene (YF, 5′-GAAGCTGTGGCA CAAAGA-3′), a 3′ primer in sequence deleted in the targeted allele (YR, 5′-ATGCAAAGGCCACACTGT-3′) and a 3′ primer internal to the *neo* insert (NR, 5′-CGACGTTAACGGTACCAA-3′).

Mouse colony maintenance. The transmitted *Yap^{tm1Smil}* allele was maintained on a mixed 129SvEv/C57BL/6J background. Crossing to an outbred (CD1; Charles River) background to obtain larger litters for embryo analyses did not perceptibly alter the phenotype of homozygous mutant embryos. Litters for phenotype characterization were generated by natural matings and staged by assigning the first half-day of embryonic development (E0.5) as noon the day of vaginal plug observation.

RT-PCR. Gene expression was assessed in wild-type embryos from blastocyst stage (E3.5) to late prenatal stage (E18.5) by RT-PCR. Positive controls for these reactions were heart or kidney cDNA libraries (Stratagene). Whole-embryo total RNA was extracted by using the TRIzol reagent (Invitrogen) according to the manufacturer's protocol with modifications for small tissue volume in embryos at ≤E10.5 as follows. (i) Embryos were dissected and rinsed several times in ice-cold phosphate-buffered saline and then transferred with a minimal volume to 40 μl of TRIzol. (ii) Embryos were homogenized by pulling through a 22-gauge 1 needle, and then the TRIzol volume was brought to 100 μl. (iii) Finally, after phase separation with the addition of 60 μl of chloroform, RNA was precipitated from the aqueous phase with 50 μl of isopropanol. cDNAs were generated according to manufacturer's protocol with the reverse transcriptase SuperScript II (Invitrogen). To test for expression of specific transcripts, we used PCR primer pairs that spanned at least one intron as follows: *Yap*, 5′-TCTGCG CAGCCAGTTGCCTA-3′ and 5′-GCTCATGCTGAGGCCGCTGT-3′; *Yap2L* (32), 5′-CCCTGATGATGTACCACTGCC-3′ and 5′-CCACTGTTAAGAAAG GGATCGG-3′; *Taz*, 5′-TCCCCAACAACTCCAGAAGAC-3′ and 5′-CAAAGT CCCGAGGTCACCAT-3′; and *loc434366*, 5′-GAATTGGAGTACAACTGGTTG TGAACAG-3′ and 5′-ACCTAATTGTGGGTATCCTTTCATTTG-3′.

In situ hybridization, immunohistochemistry, and histology. Whole-mount in situ hybridizations on dissected E6.5 to E9.5 embryos were performed essentially as described previously (61). Digoxigenin-labeled riboprobes were generated using the sequence for *Fgf8* (kindly provided by Gail Martin), *Brachyury* (T, kindly provided by Bernhard Herrmann), and α-*globin* (accession no. BC037630, I.M.A.G.E. clone 497128; Open Biosystems) fragment for sense and antisense probes subcloned into pBluescript II KS (Stratagene) using the PCR primer pairs 5′-AAACCATGGTGCTCTCTGGGGAAGA-3′ and 5′-TCTTGT GTTTCTTCCTACTCAGGCTTTATTC-3′ and *Yap* (mouse cDNA fragment subcloned into pBluescript II SK) using PCR primer pairs 5′-ACAGCCAGT GGCGTTGTCTCTG-3′ and 5′-CGGAACTATTGGTTGTCATTGTTCTCA ATTC-3′.

Whole-mount immunohistochemistry for the PECAM1 antigen followed standard methods. Primary antibody against PECAM1 (Pharmingen) was followed by horseradish peroxidase-conjugated goat anti-rat (mouse absorbed) secondary antibody (Kirkegaard and Perry Laboratories) and visualized by using a nickel-enhanced, peroxidase-based diaminobenzidine reaction.

Paraffin sections (8 to 12 μm) of embryos in utero were hematoxylin and eosin stained by using standard histological methods with fixation in 4% paraformaldehyde to allow subsequent genotyping by PCR from tissue scrapings of unstained sections of each embryo.

Protein expression analysis. Individual embryos obtained from intercross litters dissected at E8.5 and genotyped by PCR from a yolk sac tissue sample were lysed in 20 mM Tris-HCl (pH 7.4), 150 mM NaCl, 0.1% sodium dodecyl sulfate, 1% Triton X-100, 1% deoxycholic acid, and 5 mM EDTA with a cocktail of protease inhibitors. Lysates were cleared by centrifugation at 14,000 × *g* for 20

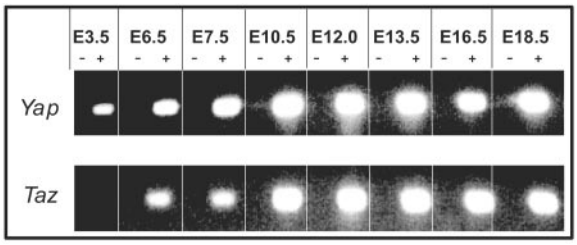

FIG. 1. *Yap* and *Taz* show widespread expression by RT-PCR across a series of mouse embryo developmental stages. PCR amplification of gene-specific products from cDNAs derived from mouse embryo total RNA obtained at E3.5, E6.5, E7.5, E10.5, E12, E13.5, E16.5, and E18.5 with (+) or without (−) RT. *Yap* expression was found at all stages examined from E3.5 blastocyst to E18.5 perinatal, in contrast to *Taz* expression, which was detected at all examined stages except E3.5 blastocyst.

min at 4°C. Protein concentrations were determined by using the BCA assay kit (Pierce Chemical Co.), and 20 μg of embryo lysate was resolved by sodium dodecyl sulfate-polyacrylamide gel electrophoresis, transferred to polyvinylidene difluoride membrane, and analyzed by Western blotting with anti-YAP 252. This antibody was generated against the C-terminal portion of human YAP and affinity purified (26). β-Actin served as a loading control.

RESULTS

Although expression of both the *Yap* and the *Taz* genes has been characterized in several cell lines and in Northern blots for both human and mouse tissue (30, 32, 45, 60, 64, 69), characterization of transcript distribution in whole tissue (39) and throughout development is lacking. To begin to explore in vivo roles for YAP, we examined expression of these genes in mouse embryos.

***Yap* expression is widespread across mouse development; *Taz* shows later onset.** We examined developmental expression of *Yap* and *Taz* by RT-PCR (Fig. 1) from blastocyst stage (E3.5) to perinatal stages (E18.5). *Yap* expression was detected at every stage examined. In addition, we examined the expression of a known mouse *Yap* splice variant in embryos from E7.5 to E18.5. Using the primer pair described previously (32), we demonstrated the expression of two *Yap* transcripts both with (Yap2L) and without the inclusion of the 48-nt (32) variant exon 6 at all developmental stages examined (data not shown). In contrast, we detected *Taz* expression at all later stages but not in blastocyst stage embryos (Fig. 1). Thus, *Yap* and *Taz* appear prevalent across mouse embryo development but show differential expression at the earliest stages.

We further explored *Yap* expression by whole mount in situ in wild-type mouse embryos from E6.5 to E8.5 (Fig. 2). Again, we found widespread *Yap* expression overall, with dynamic stage- and region-specific domains of higher relative expression. At E6.5 (Fig. 2A to D), we observed *Yap* expression throughout extraembryonic ectoderm, epiblast, and nascent mesoderm in early streak-stage embryos (Fig. 2A and B) but found at later stages (Fig. 2C) more intense expression in and adjacent to proximal epiblast regions. At E7.5 (Fig. 2E to G) we found widespread *Yap* expression with region-specific intensity distinctions (Fig. 2E and F). We observed strongest *Yap* expression in extraembryonic mesoderm and also in a ring of mid-proximodistal extraembryonic ectoderm. The strong extraembryonic ectoderm expression domain was proximal to the region forming the chorion. At this stage, *Yap* expression appeared lowest in visceral and definitive endoderm. By E8.5 (Fig. 2H,I) *Yap* expression remained widespread, with a strong expression domain at the distal tip of the allantois (Fig. 2H). Overall, we observed a nearly ubiquitous, but dynamic, *Yap* expression pattern that modulated within detectable levels across developmental stages and distinct cell types.

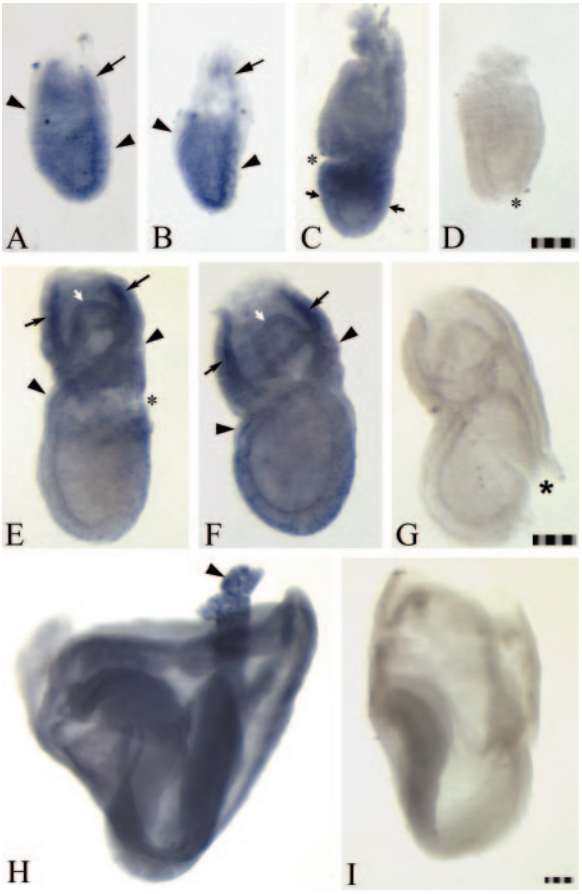

FIG. 2. Dynamic but broad *Yap* expression in wild-type mouse embryos visualized by whole mount in situ hybridization. *Yap* mRNA is broadly distributed in trophectoderm and epiblast derivatives from E6.5 to E8.5 and yet shows stage- and region-specific domains of relatively stronger expression. Control sense probes gave little background at any stage (D, G, and I). Embryos are shown with anterior to the left when known and proximal to the top. (A to D) Embryos at E6.5 showed expression in extraembryonic ectoderm (arrows in panels A and B) with high levels of *Yap* expression in epiblast becoming restricted toward proximal epiblast (above arrows in panel C) and lowest expression levels in visceral endoderm (arrowheads in panels A and B). (E to G) Embryos at E7.5 show highest expression in extraembryonic mesoderm and in a mid proximodistal domain in a ring of extraembryonic ectoderm (black arrows in panels E and F) that was proximal to the region forming the chorion (white arrows in panels E and F). Again, lowest expression levels were in visceral endoderm (arrowheads in panels E and F). (H and I) A broad *Yap* expression domain was found in embryos at E8.5 with highest expression in distal tip allantois (arrowhead in panel H). Asterisks mark regions damaged at dissection. Stage-specific scale bars, 50 μm.

Homozygous *Yap*^{tm1Smil} mutation is embryonic lethal. To define in vivo requirements for YAP, we developed a targeting construct designed to disrupt *Yap* transcription. In the targeted

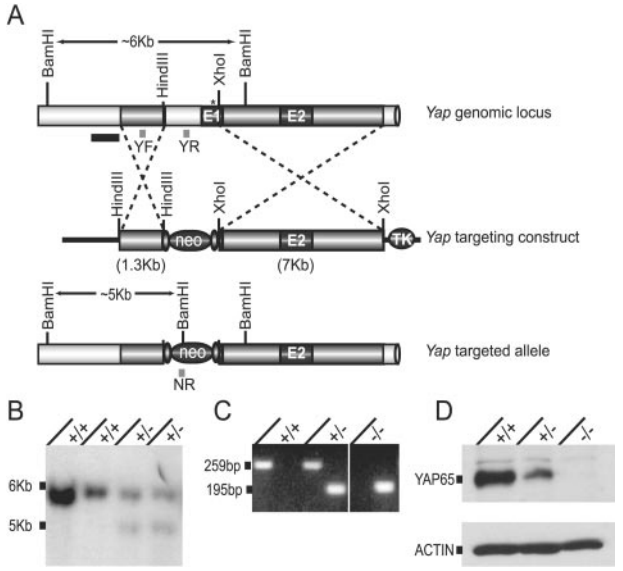

FIG. 3. Targeted disruption of the *Yap* gene. (A) The *Yap* genomic locus was altered by using a targeting vector that replaced approximately 1 kb of genomic sequence including the *Yap* ATG start site (*) and most of exon 1 with a floxed reverse orientation *MC1-neo* construct. The 3′ *PGK-tk* cassette allowed negative selection. A 5′ genomic probe (large dark bar) that recognized ~6-kb native locus and ~5-kb targeted BamHI fragments revealed proper ES cell targeting and allowed genotyping by Southern transfer. A primer trio (small bars) with a shared 5′ primer (YF) and distinct 3′ primers, one in a region deleted after targeting (YR) and the other specific for *MC1-neo* sequence (NR) allowed PCR genotyping. (B) Southern blot of ES cell DNA showing proper targeting of two ES cell lines. (C) PCR genotype of E8.5 embryos showing wild type, heterozygous, and homozygous mutant genotypes. (D) Western blot with affinity-purified rabbit polyclonal antibody to C-terminal YAP protein on E8.5 whole embryo lyses, indicating undetectable levels of YAP in homozygous mutant embryos.

allele $Yap^{tm1Smil}$ we replaced genomic sequence, including the *Yap* gene transcriptional and translational start sites and all but 10 bp of exon 1 with a reverse orientation *MC1-neo* cassette (Fig. 3A). Electroporated ES cells subjected to positive and negative selection were screened by PCR, and homologous recombination confirmed with a 5′ external probe by Southern transfer (Fig. 3B). Mice carrying the $Yap^{tm1Smil}$ allele were established by blastocyst ES cell injection and germ line transmission from chimeric founders.

Progeny from $Yap^{tm1Smil}$ heterozygous intercrosses were genotyped with PCR primer sets that generated a 259-bp product from the wild-type *Yap* allele and a 195-bp product from the $Yap^{tm1Smil}$ allele. Genotype analysis of E8.5 embryos obtained from a $Yap^{tm1Smil}$ heterozygous intercross (Fig. 3C) demonstrates the presence of all three expected genotype classes.

To assess the impact of the mutant allele on YAP protein levels, we used affinity-purified polyclonal antibody generated against carboxy-terminal human YAP (26) to probe for endogenous mouse YAP in whole-embryo lysates obtained at E8.5 from $Yap^{tm1Smil}$ intercrosses. We did not detect the 65-kDa YAP protein in homozygous mutant ($Yap^{-/-}$) embryos by Western blot analysis (Fig. 3D).

From over 900 heterozygous intercross progeny genotyped postnatally (Table 1), homozygous $Yap^{tm1Smil}$ mice were never recovered. In contrast, heterozygous mice were viable, fertile, and exhibited no overt abnormalities. To delimit the stage of embryonic lethality associated with homozygosity for $Yap^{tm1Smil}$ and to characterize the impact of YAP absence on development, we obtained embryos at several stages across the developmental timeline. From E6.5 to E9.5, we found genotype ratios consistent with the expected Mendelian distribution (Table 1, $10^2 = 2.46$, DF2). Although we genotyped two partially resorbed homozygous mutant embryos at E10.5, no $Yap^{-/-}$ embryos were recovered at later stages of development.

$Yap^{-/-}$ embryos are indistinguishable from wild type at E6.5 but show a characteristic appearance by E8.5. Although we found no distinguishing characteristics that correlated with genotype in embryos examined at E6.5 ($n = 45$ embryos; from seven litters), we did observe morphological perturbations in some mutant embryos by E7.5. By E8.5 and E9.5, however, we observed a characteristic $Yap^{-/-}$ embryo appearance (Fig. 4). Compared to wild-type siblings (Fig. 4A) at E7.5, $Yap^{-/-}$ embryos showed morphological variability ranging from overtly normal (Fig. 4B) to severely perturbed (Fig. 4C). Perturbations observed at E7.5 included very small embryos, the presence of a marked constriction at the embryonic-extraembryonic boundary (see also Fig. 5A) or complete separation of the epiblast and the extraembryonic ectoderm. We observed some morphological abnormalities in about half of the embryos analyzed at this stage. Nonetheless, most E7.5 homozygous mutant embryos were gastrulating, and many had generated a proper amnion and chorion.

In embryos from $Yap^{tm1Smil}$ heterozygous intercrosses characterized at E8.5 (Fig. 4D to G), we found $Yap^{-/-}$ embryos displayed a consistent and stereotyped morphology typified by a strikingly short and wide body axis, a distinctive multiple folding of the anterior epithelium, caudal dysgenesis, and failure of chorioallantoic attachment. Despite chorion development and allantoic extension, $Yap^{-/-}$ embryos recovered at these and later stages showed no evidence for attachment of allantois to chorion.

Among embryos recovered a E9.5 (Fig. 4H and I), $Yap^{-/-}$ embryos showed failure of ventral closure and turning, a convoluted anterior neurepithelium, and a characteristic bulbous allantois. In addition, by this stage $Yap^{-/-}$ yolk sacs had a distinctive rippled appearance.

Histological analysis indicates proper tissue type development but also yolk sac vascular defects in $Yap^{-/-}$ embryos. To provide a better understanding of developmental progression in $Yap^{-/-}$ embryos, litters from heterozygous $Yap^{tm1Smil}$ intercrosses were fixed in utero and processed for paraffin sectioning and standard hematoxylin and eosin staining (Fig. 5). Wild-

TABLE 1. Genotypes of progeny recovered from $Yap^{tm1Smil}$ intercrosses

Stage	No. of progeny			
	$Yap^{+/+}$	$Yap^{+/-}$	$Yap^{-/-}$	Total
E6.5–E9.5	59	98	52	226 (16)[a]
E10.5–E17.5	13	34	2	49[b]
Postnatal	172	318	0	490[c]

[a] Number of resorptions included in total.
[b] Resorptions not recorded.
[c] Not all male progeny were genotyped after $n = 490$; the actual number genotyped postnatally with no homozygous mutant recovery exceeds 900.

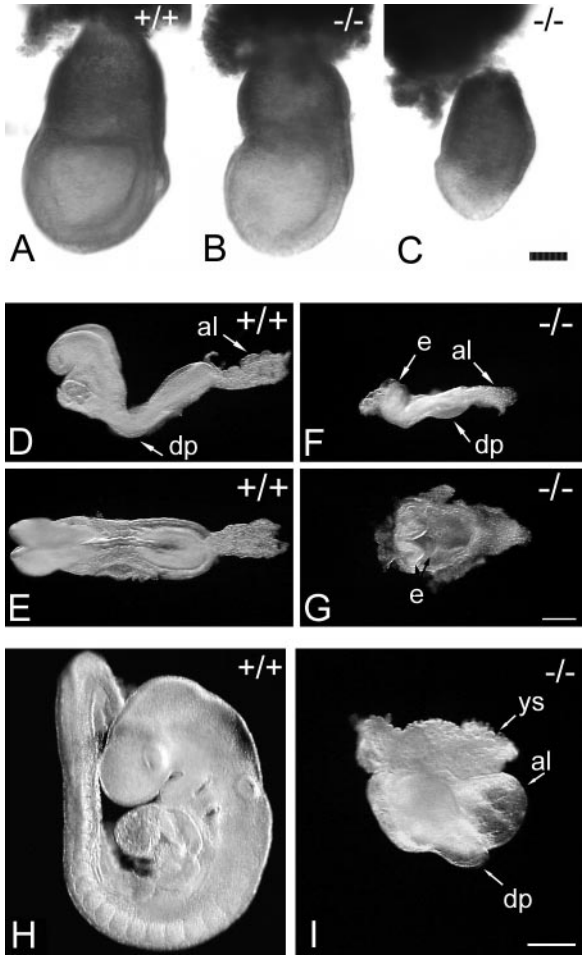

FIG. 4. Morphological phenotype of *Yap*^{tm1Smil} homozygous embryos from E7.5 to E9.5. Wild-type (A, D, E, and H) and homozygous mutant (B, C, F, G, and I) embryos from *Yap*^{tm1Smil} heterozygous intercross litters were analyzed by light microscopy for gross morphological defects. E7.5 and E8.5 embryos are with anterior to the left and proximal to the top unless otherwise noted; E9.5 embryos are shown in a left-lateral view. A comparison of wild-type (A) and homozygous mutant embryos at E7.5 revealed variability in the mutant phenotype ranging from overtly normal (B) to highly abnormal (C). At E8.5 compared to wild-type siblings (D and E), homozygous mutant embryos showed excessive folding of the anterior epithelium (e) and failure of chorioallantoic fusion despite elongation of the allantois (al). In embryos viewed from left lateral (D and F) the normal distal point (dp)—the bend point of the unturned body axis for both wild-type and homozygous mutant embryos—is indicated for comparison and illustration of caudal dysgenesis observed in mutant embryos. Comparison from a dorsal view with anterior to the left, of wild-type (E) and mutant (G) embryos clearly shows development of an abnormally short and wide axis with YAP deficiency. By E9.5, compared to wild-type siblings (H), homozygous mutant embryos (I) were much smaller and showed a stereotyped morphology that included failure of ventral closure and turning and thus retention of the distal point (dp) of earlier stages, a bulbous unfused allantois (al), and a distinctly rippled yolk sac (ys). Scale bars: 130 μm (A to C), 325 μm (D to G), and 400 μm (H and I).

type embryos sectioned at E7.5 had generated a chorion and amnion, embryonic and yolk sac mesoderm, and an allantoic bud (Fig. 5A). In addition, wild-type yolk sac mesoderm adjacent to yolk sac visceral endoderm showed cell morphology and organization consistent with early blood island development (Fig. 5B). Consistent with the morphology of dissected embryos, *Yap*$^{-/-}$ embryos sectioned at E7.5 (Fig. 5A′ and B′) had generated mesoderm but this tissue layer appeared disorganized (Fig. 5B′) relative to that of control embryos. The *Yap*$^{-/-}$ embryo shown in Fig. 5A′ and B′ demonstrated the constriction at the embryonic-extraembryonic boundary (Fig. 5A′).

We also compared stained sections from wild-type (Fig. 5C to H) and *Yap*$^{-/-}$ embryos (Fig. 5C′ to H′) at E8.5. Both wild-type and homozygous mutant embryos showed distinct chorion, amnion, and neuroectoderm development (Fig. 5C, C′, D, and D′). In wild-type embryos, the thickened epithelium of the streak region extended posterior to the node (Fig. 5C). In contrast, in *Yap*$^{-/-}$ embryos, despite development of a morphologically recognizable node (not shown), posterior regions showed a thinner tissue layer overlying the mesoderm extending to the amnion-allantoic bud junction (Fig. 5C′). This failure to maintain a posterior epiblast-like epithelium in the streak region is consistent with the observed caudal dysgenesis. In addition, anterior neurectoderm in homozygous mutant embryos showed excessive folding, extending as a single tissue layer into the amniotic cavity (Fig. 5D′). Some *Yap*$^{-/-}$ embryos developed anterior somites (Fig. 5E′) that looked much like those of wild-type sibling embryos (Fig. 5E), and some initiated heart development (Fig. 5F′) to stages similar to that of wild-type sibling embryos (Fig. 5F). Development of the *Yap*$^{-/-}$ allantois (Fig. 5G′) was similar to that of control siblings (Fig. 5G), including extension into the yolk sac cavity and differential cell morphology along the allantoic proximodistal axis. In contrast, we observed striking differences in the development of the yolk sac mesoderm. Wild-type embryos showed an easily distinguished ring of yolk sac cells organized into blood islands with the concomitant distinctions between endothelial and hematopoietic precursor cells (Fig. 5H). In *Yap*$^{-/-}$ embryos, although yolk sac mesoderm cells were abundant, well-defined blood island-like structures were rare and showed less clear cell type distinctions (Fig. 5H′).

Yolk sac but not allantoic or embryonic blood vessel formation fails in *Yap*$^{-/-}$ embryos. We used marker analysis to characterize the yolk sac vasculature defect revealed by our histological analysis. The PECAM1 antigen is a marker for endothelial precursor cells in yolk sac and mouse embryo by E8.5 (1). By E8.5, wild-type and heterozygous embryos stained with an antibody against PECAM1 (Fig. 6A to C) show a well-formed yolk sac vascular plexus, as well as allantoic and embryonic blood vessels. In sharp contrast, although *Yap*$^{-/-}$ embryos showed cells immunopositive for PECAM1, these cells entirely lacked organization into vessels in the yolk sac (Fig. 6D). Instead, PECAM1-labeled cells appeared to be profusely distributed across most of the yolk sac in homozygous mutant embryos. Conversely, the developing vasculature in the *Yap*$^{-/-}$ allantois appeared fairly normal (Fig. 6E). Although abnormally positioned, blood vessels also were evident (Fig. 6F) in the *Yap*$^{-/-}$ embryo proper. Thus, although the endothelial cell component of the early vasculature appears to be specified during *Yap*$^{-/-}$ embryogenesis, in the yolk sac endothelial cells fail to organize into vessels.

The yolk sac vasculature develops with the concomitant specification and organization of both endothelial and hematopoietic precursor cells. Early development of distinct cell

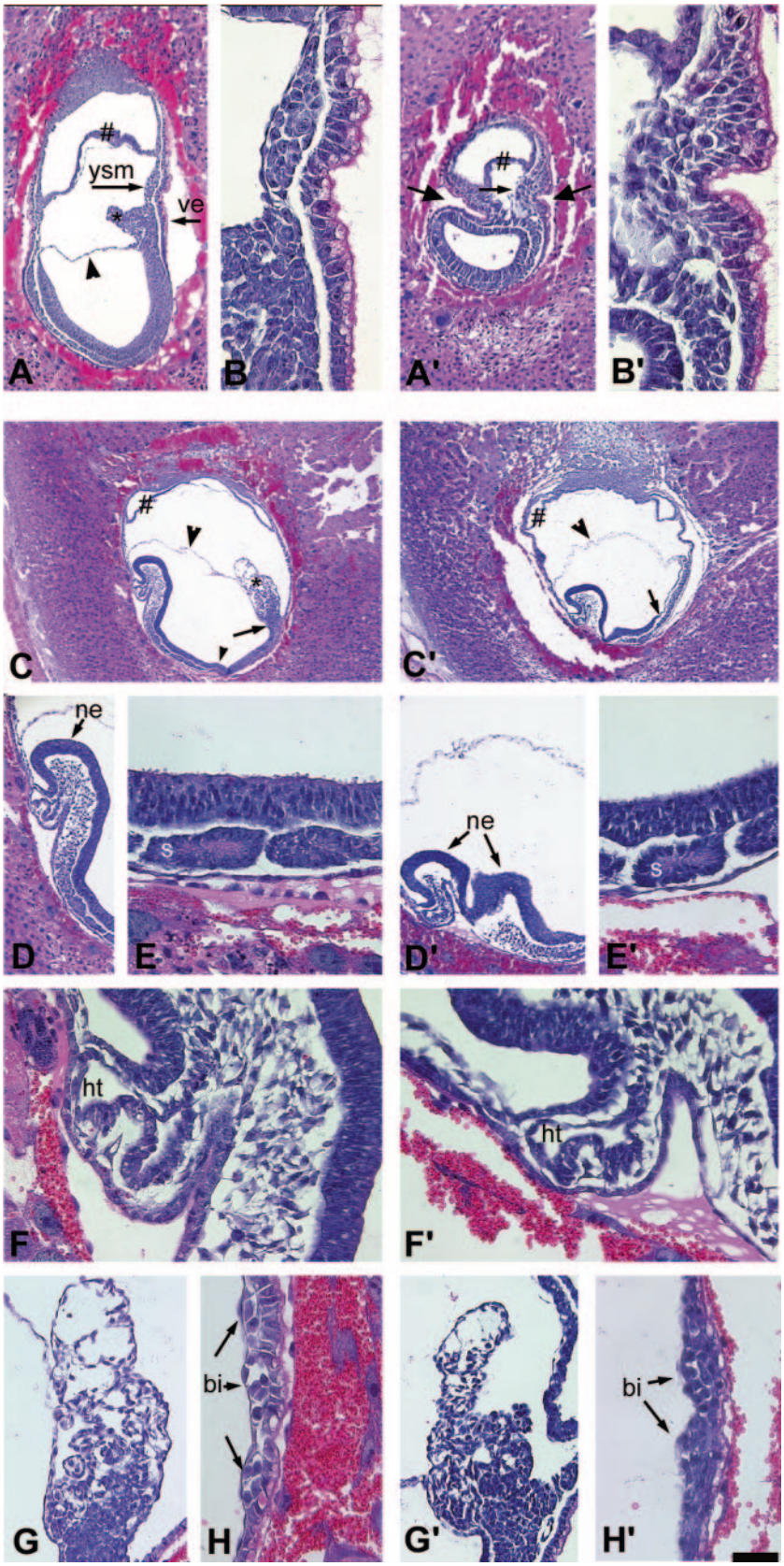

FIG. 5. Wild-type and homozygous mutant *Yap*^{tm1Smil} embryos sectioned in utero for histological analysis. Representative sections from wild-type (A to H) and homozygous mutant (A′ to H′) embryos stained with hematoxylin and eosin are shown. Unstained sections for each embryo were genotyped by PCR. By E7.5 wild-type embryos (A and B) developed chorion (#), amnion (large arrowhead) and mesoderm including the

types occurs in a ring of yolk sac tissue as organized structures referred to as blood islands which later anastomose to generate the yolk sac vascular plexus. Because our histological analysis of *Yap*$^{-/-}$ embryos showed a large number of disorganized yolk sac mesoderm cells, we explored development specifically of the hematopoietic component of the yolk sac vasculature by using a riboprobe to detect *alpha globin* expression. *Alpha globin* is expressed in erythrocyte precursors present in the murine yolk sac by E7.5 (35) and is present in these erythroblasts of the yolk sac primitive plexus at E8.5 (Fig. 6H). Whole-mount in situ analysis for *alpha globin* showed expression of this erythroblast marker in cells of the *Yap*$^{-/-}$ yolk sac (Fig. 6I to K) but in a domain lacking the distinctive organization normally observed. Thus, in *Yap*$^{-/-}$ embryos, we observe specification of both components of the early yolk sac vasculature—endothelia and erythroblasts—but see failure of these cells to develop with the organization of a proper primitive vascular plexus.

Markers for streak-tailbud, midline, and anteroposterior patterning of the neuraxis are evident despite morphological perturbation of the embryonic body axis in *Yap*$^{-/-}$ embryos. We used whole-mount in situ analyses of expression domains for several marker genes to help define the extent of patterning achieved in the *Yap*$^{-/-}$ embryo proper (Fig. 7). We used two markers, *fibroblast growth factor 8* (*Fgf8*) and *homeobox gene expressed in ES cells* (*Hesx1*) (22), to reveal the extent of anteroposterior pattern present in the convoluted neurectoderm of *Yap*$^{-/-}$ embryos by E9.5. By organogenesis stages, *Fgf8* normally is expressed in neurectoderm in both an anterior domain and at the midbrain-hindbrain boundary, in addition to branchial arch, limb bud and tail bud domains (7). Consistent with the restricted bands of expression observed in wild-type embryos (Fig. 7A), we found that *Fgf8* was present in *Yap*$^{-/-}$ embryos (Fig. 7B and C) in one or two narrow stripes across the folded neuroepithelium, indicating elements of proper AP patterning. Similarly, *Hesx1* marked the anterior-most neurepithelium (22) in both wild-type and mutant embryos (data not shown). In addition, the posterior tailbud domain showed proper *Fgf8* expression in *Yap*$^{-/-}$ embryos (Fig. 7B and C).

Because the body axis of *Yap*$^{-/-}$ embryos appears short and wide (Fig. 4F and G), we used a midline marker to assess mediolateral patterning (Fig. 7D to F). *Brachyury* (*T*) normally is expressed in the primitive streak, in the tail bud, and in the notochord precursor cells that are distributed along the midline of the embryo (62). In *Yap*$^{-/-}$ embryos (Fig. 7E and F) we found *T* expression in the streak and the tailbud. Although a *T* expression domain also demarcated a midline in *Yap*$^{-/-}$ embryos, this domain appeared unusually wide and the *T*-expressing cells were distributed in a discontinuous manner. This pattern of *T* expression suggests that *Yap*$^{-/-}$ embryos initiate midline development, specifying notochord precursor cells, but the unusual mediolateral spread and discontinuity of the *T* domain suggests abnormalities in development along the mediolateral axis, which is consistent with the abnormally wide axis morphologically evident in mutant embryos (Fig. 4G).

DISCUSSION

Embryos lacking YAP arrest development around E8.5 and display defects in yolk sac vascular development (Fig. 5H′, 6D, and H), chorioallantoic fusion (Fig. 4I), and embryonic axis elongation (Fig. 4F, G, and I). The complexity of the mutant embryo phenotype, with profound defects in both the embryo proper and the extraembryonic regions, and the observed widespread developmental *Yap* gene expression (Fig. 2) together support multiple roles for YAP in development. In general, the source of failed embryonic progression in *Yap*$^{-/-}$ embryos does not appear to result from primary problems with tissue specification since histological (Fig. 5), and marker analyses (Fig. 6 and 7) indicate relatively normal development of distinct cell types in both the yolk sac and the embryo proper. Instead, our results may reveal vital requirements for YAP in morphogenetic movements or maintenance of proper cell number during embryogenesis.

YAP is required for early steps in development of both yolk sac vasculature and placenta. One striking outcome of analyses of mouse mutant phenotypes in recent decades has been the understanding that, although profound developmental disturbances in the embryo proper may be tolerated until late gestational stages or even to birth, disruption in the cardiovascular and placental systems likely results in death in utero (4, 5, 50). Consistent with this observation, *Yap*$^{-/-}$ embryos, which die in the first half of gestation, show significant perturbation in early yolk sac vascular development, as well as in an early step in placental development. Current understanding of vascular development in the yolk sac suggests a multistep progression initiating with vasculogenesis (11). Although the molecular regulation of vasculogenesis is only beginning to be characterized (6, 11, 24), the *Vegf* signaling pathway is essential. Indeed, the vascular defect in *Yap*$^{-/-}$ yolk sac (Fig. 5 and 6) appears similar to the yolk sac phenotype of embryos that lack VEGFR1 (15) in which an overabundance of yolk sac endothelial cells underlies vasculogenesis failure (16). Although we have observed by RT-PCR retained expression of VEGFA, VEGFR1, and VEGFR2 in *Yap*$^{-/-}$ embryos (data not shown), further study may support a role for YAP along this pathway. Thus, we can now add YAP to the short list of genes known to be required for yolk sac vasculogenesis and can look for a potential role for YAP in the regulation of endothelial cell number. Strikingly, the *Yap*$^{-/-}$ embryo also pro-

allantoic bud (*) and yolk sac mesoderm (ysm), organized into early blood islands adjacent to yolk sac visceral endoderm (ve). Homozygous mutant embryos at E7.5 (A′ and B′) showed a developed chorion (#) but also variable developmental perturbations that included a pronounced constriction at the embryonic-extraembryonic boundary (large arrows) and disorganized yolk sac mesoderm (small arrow; B′). Sections at E8.5 (C to H′) show proper tissue-specific development of amnion (C and C′, arrowhead), chorion (C and C′, #), neurectoderm (D and D′), somites (E and E′), heart (F and F′), and allantois (G and G′) in both wild-type and homozygous mutant embryos. Compared to wild-type embryos, mutant embryos showed abnormal development of posterior epiblast (C and C′, small arrowhead to arrow), excessive folds of neurectoderm extending into the amniotic cavity (D and D′) and poorly defined blood islands in the yolk sac (H and H′). bi, blood island; ht, heart; s, somite; ne, neurectoderm. Scale bar: 240 μm (C and C′), 120 μm (A, A′, D, and D′), 60 μm (E, E′, G, and G′), and 30 μm (B, B′, F, F′, H, and H′).

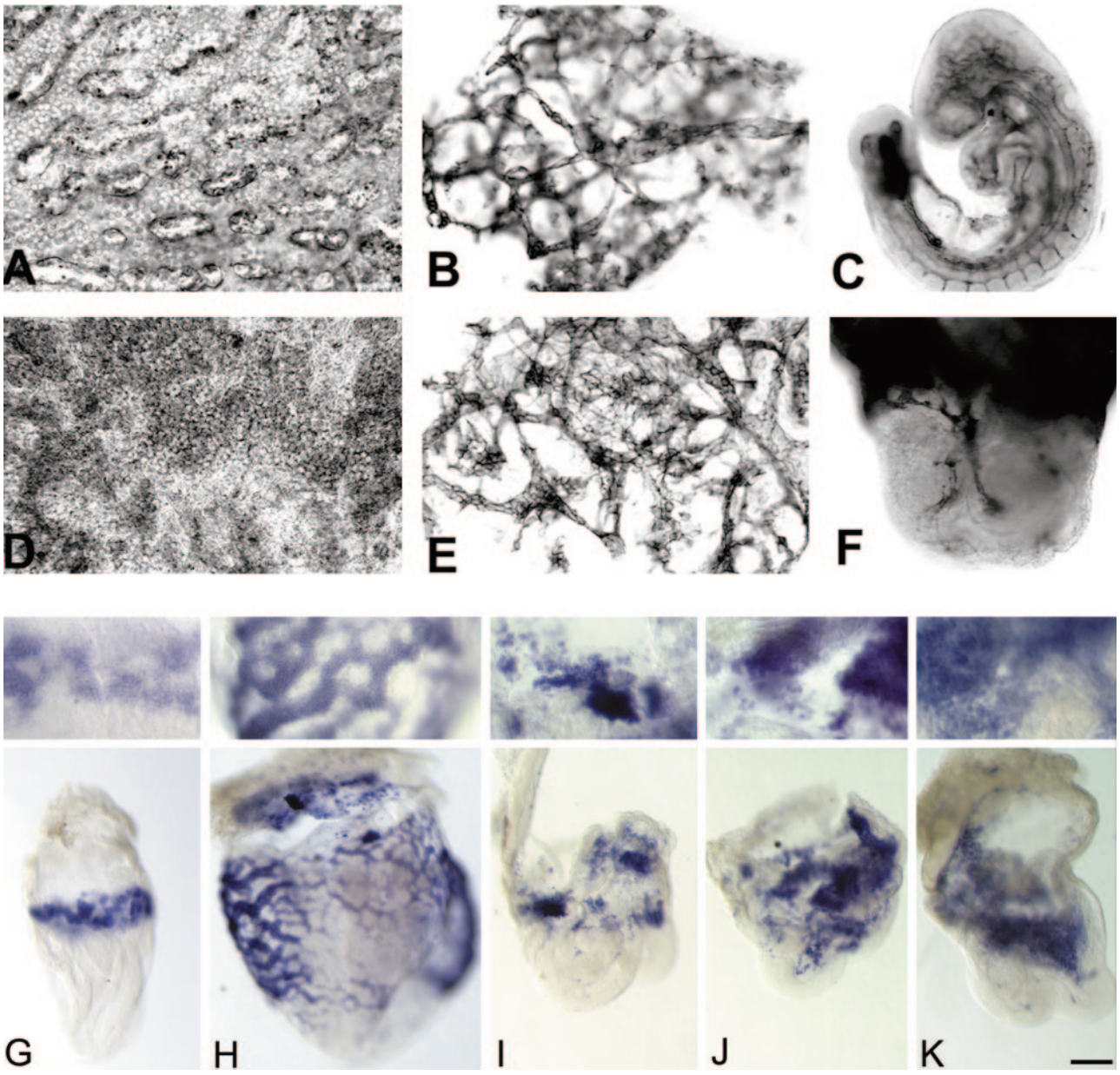

FIG. 6. Analysis of early endothelial and erythroblast markers in *Yap*^{tm1Smil} homozygous mutant embryos. Whole-mount immunohistochemical marking of PECAM1 protein (A to F) and in situ visualization of *alpha globin* expression (G to K). Endothelial cells marked by the PECAM1 antigen were present in both wild-type (A to C) and homozygous mutant (D to F) embryos late in the eighth day of development. Flat-mount images show endothelial cells organized into a primitive vascular plexus in wild-type (A) but not mutant (D) yolk sacs, where instead they showed an abundant but disordered distribution. In contrast, endothelial cells formed blood vessels in both the allantois (B and E) and the embryo proper (C and F) in both wild-type and mutant embryos. Erythroblasts expressing *alpha globin* were present in the yolk sac region of both wild-type (G and H) and homozygous mutant (I to K) embryos in the eighth day of development. In contrast to the organized early yolk sac ring of expression (G) or later intravessel distribution (H) of erythroblasts in wild-type embryos, *alpha globin*-expressing cells in mutant embryos were abundant but disordered (I to K). A higher magnification image of yolk sac is shown above each embryo image in G through K. Scale bar: 40 μm (A, B, D, E), 160 μm (C), 80 μm (F), and 250 and 100 μm (lower and upper, respectively [G to K]).

vides a genetic dissection of the process of vasculogenesis by region: in yolk sac versus in both the embryo proper and the allantois. This regional distinction corresponds largely, albeit not strictly (11), with a cellular contingent difference. In yolk sac, blood vessels develop adjacent to a visceral endoderm cell layer and, in some regions, in association with blood cell precursors. In contrast, in both embryo (11) and allantois (10) vasculogenesis proceeds largely in the absence of these other cell types. Cell-cell interactions between yolk sac mesenchyme and visceral endoderm appear to be important for yolk sac vascular development (2, 13, 46). Therefore, it may be that the role of YAP lies in the cross talk between yolk sac mesenchyme and adjacent yolk sac visceral endoderm. Alternatively, YAP may mediate steps essential for vessel development specifically

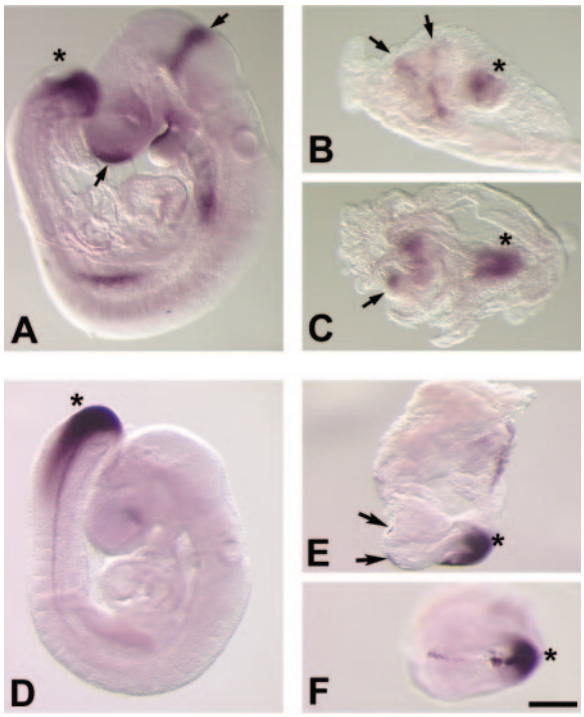

FIG. 7. Whole-mount in situ analyses of *Yap65*^{tm1Smil} homozygous mutant embryos with postgastrulation markers of body axis development. Anteroposterior pattern was revealed by restricted domains for *Fgf8* (A to C) at E9.5. Homozygous mutant embryos showed one or two stripes of *Fgf8* expression (B and C, arrows) consistent with the restricted neurectoderm expression domains in wild-type sibling embryos. The streak/tailbud region is marked by both *Fgf8* (A to C, asterisk) and *Brachyury* (*T*; D to F, asterisk) in both wild-type (A and D) and homozygous mutant (B, C, E, and F) embryos. Mutant embryos show an abnormally discontinuous (E, arrows) and broad (F) *Brachyury* expression domain in midline cells compared to wild-type embryos. Scale bar: 325 μm (A to C, F to H), 290 μm (D), and 145 μm (E).

in the presence of hematopoietic precursors, a developmental process that remains largely uncharacterized.

YAP also appears fundamental to an early step in placental development: attachment of the allantois to the chorion. The bulbous appearance of the *Yap*$^{-/-}$ allantois by E9.5 (Fig. 4I) is like that observed in other embryos in which the allantois forms and elongates but fails to fuse with the chorion (20, 28, 33, 34, 36, 42, 44, 48, 50, 52, 56, 59, 63, 67). We found that *Yap* is expressed in the cell components potentially involved in the process (9) including chorionic ectoderm, chorionic mesoderm, and allantois (Fig. 2E, F, and H). In addition, we observed proper initial development of these tissue types in mutant embryos, suggesting again that YAP functions not generally for cell type specification but principally in the cell-cell interaction events required for attachment. The apparent higher intensity *Yap* expression in distal-tip allantois (Fig. 2H)—the very region required for initial attachment—motivates further study. Curiously, for many of the genes with identified roles in chorioallantoic attachment and fusion, mutation causes defects in this process in only a fraction of the homozygous mutant embryos. This observation supports the existence of multiple pathways to reach fusion, each of which may sometimes suffice alone. Remarkably, we found failed chorioallantoic attachment in 100% of *Yap*$^{-/-}$ embryos observed. Therefore, YAP appears fundamental to this critical step in the initiation of the placental circulation.

YAP plays a role in shaping the embryonic body axis. In addition to showing critical requirements for YAP in early steps of yolk sac vascular and placental development, *Yap*$^{-/-}$ embryos also reveal an essential role for YAP in shaping the main body axis of the embryo. Failure to elongate the body axis in *Yap*$^{-/-}$ embryos suggests a role for YAP in the regulation of cell number in the embryo proper and/or in the fundamental morphogenetic movements of gastrulation. We found that the *Yap*$^{-/-}$ embryo phenotype overall appeared remarkably similar to that shown by mouse embryos carrying mutations influencing fibronectin (FN)-$\alpha_5\beta_1$ integrin interactions (17–19, 66, 68). Indeed, mouse embryos in which FN-$\alpha_5\beta_1$ interactions have been perturbed show a short, wide body axis, and yolk sac vascular defects as do *Yap* mutant embryos. Moreover, the YAP binding partners of the Src kinase family have been shown to mediate integrin-stimulated cell migration (41) and mouse embryos triple mutant for three of these genes—*Src*, c-*Yes*, and *Fyn*—also show a shortened body axis similar to the FN-$\alpha_5\beta_1$ mutant classes (31) and thus also to *Yap* mutant embryos. Furthermore, a possible role for YAP in the convergent extension cell movements critical for vertebrate body axis elongation is suggested by evidence of a role for the zebra fish *Fyn* and c-*Yes* homologs in this process (29). Thus, YAP might serve by several potential interactions to promote the morphogenetic movements critical for proper axis elongation.

In addition, YAP could impact axis elongation through the regulation of proliferation, apoptosis, or both processes. Indeed, YAP is known by biochemical and cell culture assays to influence apoptotic and cell cycle regulatory pathways (12, 55). Moreover, recent evidence from *Drosophila* supports a role for YAP in regulating these processes (27). Nonetheless, the available genetic evidence from mice indicates that these known interactions alone are insufficient to explain the phenotype since, for example, mouse embryos homozygous mutant for either *p73* (65) or *p63* (40) survive to birth. Although not characterized extensively in wild-type gastrula-stage mouse embryos, apoptosis and proliferation appear to be fairly evenly distributed with potentially higher rates of both processes associated with distal and anterior epiblast (23, 38, 49, 51, 53, 54, 58). Although we are in the process of rigorously examining both proliferation and apoptosis in the absence of YAP, our histological preparations of E7.5 *Yap*$^{-/-}$ embryos (Fig. 5A′ and B′) do not suggest marked changes in the number of mitotic or dying cells. At later stages, with more perturbed mutant embryo development, it becomes difficult to distinguish primary from secondary impacts on cell survival and proliferation.

A critical developmental requirement for YAP is not compensated for by TAZ expression. We observe expression of both *Yap* and *Taz* throughout most of mouse embryo development, with differential expression observed only at the blastocyst stage (Fig. 1). Despite this predominantly concomitant expression and our finding by RT-PCR analysis of retained *Taz* expression in mutant embryos (data not shown), *Yap*$^{-/-}$ embryos show severe developmental perturbation. This result argues for critical requirements for YAP that cannot be compensated for by potential redundant functions of the related protein TAZ. Possibly, a single time window for this vital YAP role occurs at peri-implantation stages, prior to TAZ expres-

sion onset. Nonetheless, it seems likely that YAP plays many roles throughout development some of which will occur during concomitant TAZ expression. Thus, the phenotype of the mutant embryo supports unique in vivo requirements for YAP. Teasing apart the mechanisms of YAP function in development may provide insight into the rules defining the independent roles of these related proteins.

The study of YAP interactions and function in vitro and in cell culture has identified several binding partners and potential signaling pathway interactions for this protein. We generated a targeted null allele to reveal YAP requirements at the level of the whole organism. We found that the *Yap*$^{-/-}$ phenotype overall is not easily accounted for by individual interactions with known binding partners or signaling pathways. This result may be explained to some extent by combinatorial effects, with multiple YAP interactions impacting embryogenesis. These observations also may suggest, however, that protein-protein interactions between YAP and heretofore unrecognized binding partners could play critical roles in the early stages of embryogenesis.

ACKNOWLEDGMENTS

We thank Stephen Gee for critical reading of the manuscript, Sean Barron for help with mouse colony maintenance, the UNC Histopathology Facility for sections, and the UNC Animal Models Core for generating *Yap*^{tm1Smil} chimeric founders.

This study was supported by National Institutes of Health grant HL63755 to S.L.M.

REFERENCES

1. **Baldwin, H. S., H. M. Shen, H. C. Yan, H. M. DeLisser, A. Chung, C. Mickanin, T. Trask, N. E. Kirschbaum, P. J. Newman, S. M. Albelda, et al.** 1994. Platelet endothelial cell adhesion molecule-1 (PECAM-1/CD31): alternatively spliced, functionally distinct isoforms expressed during mammalian cardiovascular development. Development **120:**2539–2553.
2. **Baron, M. H.** 2001. Induction of embryonic hematopoietic and endothelial stem/progenitor cells by hedgehog-mediated signals. Differentiation **68:**175–185.
3. **Basu, S., N. F. Totty, M. S. Irwin, M. Sudol, and J. Downward.** 2003. Akt phosphorylates the Yes-associated protein, YAP, to induce interaction with 14-3-3 and attenuation of p73-mediated apoptosis. Mol. Cell **11:**11–23.
4. **Conway, S. J., A. Kruzynska-Frejtag, P. L. Kneer, M. Machnicki, and S. V. Koushik.** 2003. What cardiovascular defect does my prenatal mouse mutant have, and why? Genesis **35:**1–21.
5. **Copp, A. J.** 1995. Death before birth: clues from gene knockouts and mutations. Trends Genet. **11:**87–93.
6. **Crosby, C. V., P. A. Fleming, W. S. Argraves, M. Corada, L. Zanetta, E. Dejana, and C. J. Drake.** 2005. VE-cadherin is not required for the formation of nascent blood vessels but acts to prevent their disassembly. Blood **105:**2771–2776.
7. **Crossley, P. H., and G. R. Martin.** 1995. The mouse Fgf8 gene encodes a family of polypeptides and is expressed in regions that direct outgrowth and patterning in the developing embryo. Development **121:**439–451.
8. **Cui, C. B., L. F. Cooper, X. Yang, G. Karsenty, and I. Aukhil.** 2003. Transcriptional coactivation of bone-specific transcription factor Cbfa1 by TAZ. Mol. Cell. Biol. **23:**1004–1013.
9. **Downs, K. M.** 2002. Early placental ontogeny in the mouse. Placenta **23:** 116–131.
10. **Downs, K. M., S. Gifford, M. Blahnik, and R. L. Gardner.** 1998. Vascularization in the murine allantois occurs by vasculogenesis without accompanying erythropoiesis. Development **125:**4507–4520.
11. **Drake, C. J.** 2003. Embryonic and adult vasculogenesis. Birth Defects Res. C Embryo Today **69:**73–82.
12. **Espanel, X., and M. Sudol.** 2001. Yes-associated protein and p53-binding protein-2 interact through their WW and SH3 domains. J. Biol. Chem. **276:**14514–14523.
13. **Farrington, S. M., M. Belaoussoff, and M. H. Baron.** 1997. Winged-helix, Hedgehog, and Bmp genes are differentially expressed in distinct cell layers of the murine yolk sac. Mech. Dev. **62:**197–211.
14. **Ferrigno, O., F. Lallemand, F. Verrecchia, S. L'Hoste, J. Camonis, A. Atfi, and A. Mauviel.** 2002. Yes-associated protein (YAP65) interacts with Smad7 and potentiates its inhibitory activity against TGF-β/Smad signaling. Oncogene **21:**4879–4884.
15. **Fong, G. H., J. Rossant, M. Gertsenstein, and M. L. Breitman.** 1995. Role of the Flt-1 receptor tyrosine kinase in regulating the assembly of vascular endothelium. Nature **376:**66–70.
16. **Fong, G. H., L. Zhang, D. M. Bryce, and J. Peng.** 1999. Increased hemangioblast commitment, not vascular disorganization, is the primary defect in flt-1 knockout mice. Development **126:**3015–3025.
17. **George, E. L., H. S. Baldwin, and R. O. Hynes.** 1997. Fibronectins are essential for heart and blood vessel morphogenesis but are dispensable for initial specification of precursor cells. Blood **90:**3073–3081.
18. **George, E. L., E. N. Georges-Labouesse, R. S. Patel-King, H. Rayburn, and R. O. Hynes.** 1993. Defects in mesoderm, neural tube, and vascular development in mouse embryos lacking fibronectin. Development **119:**1079–1091.
19. **Goh, K. L., J. T. Yang, and R. O. Hynes.** 1997. Mesodermal defects and cranial neural crest apoptosis in alpha5 integrin-null embryos. Development **124:**4309–4319.
20. **Gurtner, G. C., V. Davis, H. Li, M. J. McCoy, A. Sharpe, and M. I. Cybulsky.** 1995. Targeted disruption of the murine VCAM1 gene: essential role of VCAM-1 in chorioallantoic fusion and placentation. Genes Dev. **9:**1–14.
21. **Harris, B. Z., and W. A. Lim.** 2001. Mechanism and role of PDZ domains in signaling complex assembly. J. Cell Sci. **114:**3219–3231.
22. **Hermesz, E., S. Mackem, and K. A. Mahon.** 1996. Rpx: a novel anterior-restricted homeobox gene progressively activated in the prechordal plate, anterior neural plate and Rathke's pouch of the mouse embryo. Development **122:**41–52.
23. **Heyer, B. S., A. MacAuley, O. Behrendtsen, and Z. Werb.** 2000. Hypersensitivity to DNA damage leads to increased apoptosis during early mouse development. Genes Dev. **14:**2072–2084.
24. **Hiratsuka, S., K. Nakao, K. Nakamura, M. Katsuki, Y. Maru, and M. Shibuya.** 2005. Membrane fixation of vascular endothelial growth factor receptor 1 ligand-binding domain is important for vasculogenesis and angiogenesis in mice. Mol. Cell. Biol. **25:**346–354.
25. **Hong, J. H., E. S. Hwang, M. T. McManus, A. Amsterdam, Y. Tian, R. Kalmukova, E. Mueller, T. Benjamin, B. M. Spiegelman, P. A. Sharp, N. Hopkins, and M. B. Yaffe.** 2005. TAZ, a transcriptional modulator of mesenchymal stem cell differentiation. Science **309:**1074–1078.
26. **Howell, M., C. Borchers, and S. L. Milgram.** 2004. Heterogeneous nuclear ribonuclear protein U associates with YAP and regulates its coactivation of Bax transcription. J. Biol. Chem. **279:**26300–26306.
27. **Huang, J., S. Wu, J. Barrera, K. Matthews, and D. Pan.** 2005. The Hippo signaling pathway coordinately regulates cell proliferation and apoptosis by inactivating Yorkie, the *Drosophila* homolog of YAP. Cell **122:**421–434.
28. **Hunter, P. J., B. J. Swanson, M. A. Haendel, G. E. Lyons, and J. C. Cross.** 1999. Mrj encodes a DnaJ-related co-chaperone that is essential for murine placental development. Development **126:**1247–1258.
29. **Jopling, C., and J. den Hertog.** 2005. Fyn/Yes and non-canonical Wnt signalling converge on RhoA in vertebrate gastrulation cell movements. EMBO Rep. **6:**426–431.
30. **Kanai, F., P. A. Marignani, D. Sarbassova, R. Yagi, R. A. Hall, M. Donowitz, A. Hisaminato, T. Fujiwara, Y. Ito, L. C. Cantley, and M. B. Yaffe.** 2000. TAZ: a novel transcriptional coactivator regulated by interactions with 14-3-3 and PDZ domain proteins. EMBO J. **19:**6778–6791.
31. **Klinghoffer, R. A., C. Sachsenmaier, J. A. Cooper, and P. Soriano.** 1999. Src family kinases are required for integrin but not PDGFR signal transduction. EMBO J. **18:**2459–2471.
32. **Komuro, A., M. Nagai, N. E. Navin, and M. Sudol.** 2003. WW domain-containing protein YAP associates with ErbB-4 and acts as a co-transcriptional activator for the carboxyl-terminal fragment of ErbB-4 that translocates to the nucleus. J. Biol. Chem. **278:**33334–33341.
33. **Kwee, L., H. S. Baldwin, H. M. Shen, C. L. Stewart, C. Buck, C. A. Buck, and M. A. Labow.** 1995. Defective development of the embryonic and extraembryonic circulatory systems in vascular cell adhesion molecule (VCAM-1) deficient mice. Development **121:**489–503.
34. **Lechleider, R. J., J. L. Ryan, L. Garrett, C. Eng, C. Deng, A. Wynshaw-Boris, and A. B. Roberts.** 2001. Targeted mutagenesis of Smad1 reveals an essential role in chorioallantoic fusion. Dev. Biol. **240:**157–167.
35. **Leder, A., A. Kuo, M. M. Shen, and P. Leder.** 1992. In situ hybridization reveals coexpression of embryonic and adult alpha globin genes in the earliest murine erythrocyte progenitors. Development **116:**1041–1049.
36. **Mahlapuu, M., M. Ormestad, S. Enerback, and P. Carlsson.** 2001. The forkhead transcription factor Foxf1 is required for differentiation of extraembryonic and lateral plate mesoderm. Development **128:**155–166.
37. **Mahoney, W. M., J. H. Hong, M. B. Yaffe, and I. K. Farrance.** 2005. The transcriptional coactivator TAZ interacts differentially with transcriptional enhancer factor-1 (TEF-1) family members. Biochem. J. **388:**217–225.
38. **Manova, K., C. Tomihara-Newberger, S. Wang, A. Godelman, S. Kalantry, K. Witty-Blease, V. De Leon, W. S. Chen, E. Lacy, and R. F. Bachvarova.** 1998. Apoptosis in mouse embryos: elevated levels in pregastrulae and in the distal anterior region of gastrulae of normal and mutant mice. Dev. Dyn. **213:**293–308.
39. **Milewski, R. C., N. C. Chi, J. Li, C. Brown, M. M. Lu, and J. A. Epstein.** 2004. Identification of minimal enhancer elements sufficient for Pax3 expres-

sion in neural crest and implication of Tead2 as a regulator of Pax3. Development **131:**829–837.
40. **Mills, A. A., B. Zheng, X. J. Wang, H. Vogel, D. R. Roop, and A. Bradley.** 1999. p63 is a p53 homologue required for limb and epidermal morphogenesis. Nature **398:**708–713.
41. **Mitra, S. K., D. A. Hanson, and D. D. Schlaepfer.** 2005. Focal adhesion kinase: in command and control of cell motility. Nat. Rev. Mol. Cell. Biol. **6:**56–68.
42. **Mo, F. E., A. G. Muntean, C. C. Chen, D. B. Stolz, S. C. Watkins, and L. F. Lau.** 2002. CYR61 (CCN1) is essential for placental development and vascular integrity. Mol. Cell. Biol. **22:**8709–8720.
43. **Mohler, P. J., S. M. Kreda, R. C. Boucher, M. Sudol, M. J. Stutts, and S. L. Milgram.** 1999. Yes-associated protein 65 localizes p62(c-Yes) to the apical compartment of airway epithelia by association with EBP50. J. Cell Biol. **147:**879–890.
44. **Naiche, L. A., and V. E. Papaioannou.** 2003. Loss of Tbx4 blocks hindlimb development and affects vascularization and fusion of the allantois. Development **130:**2681–2693.
45. **Omerovic, J., E. M. Puggioni, S. Napoletano, V. Visco, R. Fraioli, L. Frati, A. Gulino, and M. Alimandi.** 2004. Ligand-regulated association of ErbB-4 to the transcriptional coactivator YAP65 controls transcription at the nuclear level. Exp. Cell Res. **294:**469–479.
46. **Palis, J., K. E. McGrath, and P. D. Kingsley.** 1995. Initiation of hematopoiesis and vasculogenesis in murine yolk sac explants. Blood **86:**156–163.
47. **Park, K. S., J. A. Whitsett, T. Di Palma, J. H. Hong, M. B. Yaffe, and M. Zannini.** 2004. TAZ interacts with TTF-1 and regulates expression of surfactant protein-C. J. Biol. Chem. **279:**17384–17390.
48. **Parr, B. A., V. A. Cornish, M. I. Cybulsky, and A. P. McMahon.** 2001. Wnt7b regulates placental development in mice. Dev. Biol. **237:**324–332.
49. **Poelmann, R. E.** 1980. Differential mitosis and degeneration patterns in relation to the alterations in the shape of the embryonic ectoderm of early post-implantation mouse embryos. J. Embryol. Exp. Morphol. **55:**33–51.
50. **Rossant, J., and J. C. Cross.** 2001. Placental development: lessons from mouse mutants. Nat. Rev. Genet. **2:**538–548.
51. **Sanders, E. J., P. H. Torkkeli, and A. S. French.** 1997. Patterns of cell death during gastrulation in chick and mouse embryos. Anat. Embryol. **195:**147–154.
52. **Saunders, D. N., S. L. Hird, S. L. Withington, S. L. Dunwoodie, M. J. Henderson, C. Biben, R. L. Sutherland, C. J. Ormandy, and C. K. Watts.** 2004. Edd, the murine hyperplastic disc gene, is essential for yolk sac vascularization and chorioallantoic fusion. Mol. Cell. Biol. **24:**7225–7234.
53. **Snow, M. H. L.** 1977. Gastrulation in the mouse: growth and regionalisation of the epiblast. J. Embryol. Exp. Morphol. **42:**293–303.
54. **Solter, D., N. Skreb, and I. Damjanov.** 1971. Cell cycle analysis in the mouse EGG-cylinder. Exp. Cell Res. **64:**331–334.
55. **Strano, S., E. Munarriz, M. Rossi, L. Castagnoli, Y. Shaul, A. Sacchi, M. Oren, M. Sudol, G. Cesareni, and G. Blandino.** 2001. Physical interaction with Yes-associated protein enhances p73 transcriptional activity. J. Biol. Chem. **276:**15164–15173.
56. **Stumpo, D. J., N. A. Byrd, R. S. Phillips, S. Ghosh, R. R. Maronpot, T. Castranio, E. N. Meyers, Y. Mishina, and P. J. Blackshear.** 2004. Chorioallantoic fusion defects and embryonic lethality resulting from disruption of Zfp36L1, a gene encoding a CCCH tandem zinc finger protein of the Tristetraprolin family. Mol. Cell. Biol. **24:**6445–6455.
57. **Sudol, M.** 1994. Yes-associated protein (YAP65) is a proline-rich phosphoprotein that binds to the SH3 domain of the Yes proto-oncogene product. Oncogene **9:**2145–2152.
58. **Tebbs, R. S., M. L. Flannery, J. J. Meneses, A. Hartmann, J. D. Tucker, L. H. Thompson, J. E. Cleaver, and R. A. Pedersen.** 1999. Requirement for the Xrcc1 DNA base excision repair gene during early mouse development. Dev. Biol. **208:**513–529.
59. **Tremblay, K. D., N. R. Dunn, and E. J. Robertson.** 2001. Mouse embryos lacking Smad1 signals display defects in extra-embryonic tissues and germ cell formation. Development **128:**3609–3621.
60. **Vassilev, A., K. J. Kaneko, H. Shu, Y. Zhao, and M. L. DePamphilis.** 2001. TEAD/TEF transcription factors utilize the activation domain of YAP65, a Src/Yes-associated protein localized in the cytoplasm. Genes Dev. **15:**1229–1241.
61. **Wilkinson, D. G.** 1992. In situ hybridization: a practical approach. IRL Press at Oxford University Press, Oxford, N.Y.
62. **Wilkinson, D. G., S. Bhatt, and B. G. Herrmann.** 1990. Expression pattern of the mouse T gene and its role in mesoderm formation. Nature **343:**657–659.
63. **Xu, X., M. Weinstein, C. Li, M. Naski, R. I. Cohen, D. M. Ornitz, P. Leder, and C. Deng.** 1998. Fibroblast growth factor receptor 2 (FGFR2)-mediated reciprocal regulation loop between FGF8 and FGF10 is essential for limb induction. Development **125:**753–765.
64. **Yagi, R., L. F. Chen, K. Shigesada, Y. Murakami, and Y. Ito.** 1999. A WW domain-containing yes-associated protein (YAP) is a novel transcriptional coactivator. EMBO J. **18:**2551–2562.
65. **Yang, A., N. Walker, R. Bronson, M. Kaghad, M. Oosterwegel, J. Bonnin, C. Vagner, H. Bonnet, P. Dikkes, A. Sharpe, F. McKeon, and D. Caput.** 2000. p73-deficient mice have neurological, pheromonal and inflammatory defects but lack spontaneous tumours. Nature **404:**99–103.
66. **Yang, J. T., B. L. Bader, J. A. Kreidberg, M. Ullman-Cullere, J. E. Trevithick, and R. O. Hynes.** 1999. Overlapping and independent functions of fibronectin receptor integrins in early mesodermal development. Dev. Biol. **215:**264–277.
67. **Yang, J. T., H. Rayburn, and R. O. Hynes.** 1995. Cell adhesion events mediated by alpha 4 integrins are essential in placental and cardiac development. Development **121:**549–560.
68. **Yang, J. T., H. Rayburn, and R. O. Hynes.** 1993. Embryonic mesodermal defects in alpha 5 integrin-deficient mice. Development **119:**1093–1105.
69. **Zaidi, S. K., A. J. Sullivan, R. Medina, Y. Ito, A. J. Van Wijnen, J. L. Stein, J. B. Lian, and G. S. Stein.** 2004. Tyrosine phosphorylation controls Runx2-mediated subnuclear targeting of YAP to repress transcription. EMBO J. **23:**790–799.